Hydrogen mass transport resistance changes in a high temperature polymer membrane fuel cell as a function of current density and acid doping

Thomas, Sobi; Araya, Samuel Simon; Frensch, Steffen Henrik; Steenberg, Thomas; Kær, Søren Knudsen

Published in:
Electrochimica Acta

DOI (link to publication from Publisher):
10.1016/j.electacta.2019.06.021

Publication date:
2019

Document Version
Accepted author manuscript, peer reviewed version

Accepted Manuscript

Hydrogen mass transport resistance changes in a high temperature polymer membrane fuel cell as a function of current density and acid doping

Sobi Thomas, Samuel Simon Araya, Steffen Henrik Frensch, Thomas Steenberg, Søren Knudsen Kær

PII: S0013-4686(19)31164-8

DOI: https://doi.org/10.1016/j.electacta.2019.06.021

Reference: EA 34328

To appear in: *Electrochimica Acta*

Received Date: 19 September 2018

Revised Date: 14 May 2019

Accepted Date: 4 June 2019

Please cite this article as: S. Thomas, S.S. Araya, S.H. Frensch, T. Steenberg, Sø.Knudsen. Kær, Hydrogen mass transport resistance changes in a high temperature polymer membrane fuel cell as a function of current density and acid doping, *Electrochimica Acta* (2019), doi: https://doi.org/10.1016/j.electacta.2019.06.021.

Hydrogen mass transport resistance changes in a high temperature polymer membrane fuel cell as a function of current density and acid doping

Sobi Thomas[a,*], Samuel Simon Araya[a], Steffen Henrik Frensch[a], Thomas Steenberg[b], Søren Knudsen Kær[a,*]

[a]*Department of Energy Technology, Pontoppidanstræde, Aalborg University, Aalborg East -9220, Denmark*
[b]*Danish Power Systems, Egeskowej 6c, DK-3490 Kvistgaard, Denmark*

Abstract

High temperature polymer electrolyte membrane fuel cells (HT-PEMFC) have phosphoric acid doped membranes. Acid in the membrane is mobile and tends to move out of the membrane depending on the acid doping. The migration of acid (when the doping is high) towards the anode at high current density > 0.4 A cm^{-2} causes gas diffusion layer (GDL) and catalyst flooding which thereby results higher hydrogen transport resistance. Thus, it is important to determine the acid doping level, which is optimal. In this study, transient changes in hydrogen mass transport is investigated as a function of doping level and current density. Three doping levels 11, 8.3 and 7 molecules of H_3PO_4 per PBI repeat unit are investigated. Electrochemical impedance spectroscopy (EIS) was modified to a single frequency measurement and time constant are calculated for resistance change with current density using a linear fit. The time constants are 2.0±0.5, 3.4±0.3, 8.2±0.2 min for low and 2.5±0.8, 4.9±0.3 and 4.5±0.2 min for high current densities, for the respective doping levels. The resistance decreases at high and increases at low current densities for all the doping levels with a varying time constant. This change in time constant is attributed to low doping level having lower capillary pressure to push the acid from reaching GDL pores from the membrane and/or catalyst layer.

Keywords: Load cycling, EIS, Fuel cell, high temperature PEM, Phosphoric acid

1. Introduction

High temperature PEM fuel cells (HT-PEMFC) have several advantages in terms of higher CO tolerance and minimal humidification complexities [1, 2]. The most commonly used membrane is phosphoric acid doped polybenzimidazole (PBI) membranes. The advantage is the possibility of fuel cell operation at elevated temperatures which enhances the reaction kinetics and reduces engineering problems associated with system design. HT-PEM fuel cells are operated at a temperature of around 160-180 °C. The proton conductors in these fuel cells are phosphoric acid (PA) which makes the fuel cell operation at elevated temperature possible without humidification. However, the presence of acid required for the proton conduction is also associated with some problems. The PBI matrix which is doped with PA takes up two acid molecules per PBI repetitive unit. However, the acid doping required to achieve reasonable performance is significantly higher. The doping level also depends on the membrane preparation method. Two most commonly used MEAs in HT-PEM fuel cells are sol-gel type and post-doped MEAs. In case of sol-gel MEAs, the acid doping level can reach up to 70 per PBI repeat unit [1] and is much higher compared to post-doped MEAs which usually have doping level of 9-12 per PBI repeat unit [3]. .

Nevertheless, in both the cases, a large amount of acid is free within the cell and can move to other parts of the cell, such as the gas diffusion layer (GDL), catalyst layer and also the flow-plates, from where the chances of it getting removed with the gases are high. The loss of phosphoric acid is a highly debated topic considering the fact that differently doped MEAs as mentioned above are available commercially. Some authors reported that there is a loss of acid by evaporation which leads to the degradation of HT-PEMFC in the long term when the doping is high [4, 5]. The other argument reported is that the acid loss is not an issue for the durability under certain operating conditions [6, 7].

Yu et al. [7] investigated the cause of degradation in an HT-PEMFC using continuous 550 h operation. The test results show a degradation rate of 0.18 mV h^{-1} after an activation for 90 h. The analysis based on different characterization methods suggest that the degradation was a result of catalyst agglomeration and thereby leading to acid leaching from the catalyst and getting lost. The investigation of acid redistribution on an operating HT-PEM fuel cell was carried out as a function of current density. When a load (140 mA cm^{-2}) was applied, the membrane was seen to swell by ≈20% compared to operating at open circuit voltage (OCV). This increase was attributed to an increment in the water generated which gets attracted by the PA. Further increment of current density to 550 mA cm^{-2} did not further increase the membrane thickness [8]. The lifetime investigation of HT-PEM fuel cell under accelerated stress test was investigated by [5]. The parameters considered which

*Corresponding author
Email addresses: sot@et.aau.dk (Sobi Thomas), skk@et.aau.dk (Søren Knudsen Kær)

could influence the acid loss were temperature and reactant flow rates. They reported 40% loss in acid from a beginning doping level of ≈36 molecules of H_3PO_4 per PBI repeat unit resulted in minimal loss of performance. They also reported that the rate of acid loss over a period of 2830 h up to a PA loss of 90 % was same. They suggested there was no effect on the rate of acid loss to the MEA doping levels [5].

Maier et al. [8] reported 20 % of generated water on the cathode migrates to the anode under the influence of differences in acid concentration and PA affinity for water. In different studies using nuclear magnetic resonance (NMR) spectroscopy [9, 10] it was reported that the proton conductivity in PA-doped PBI membrane is dominated by H_3O^+ and H_2O species at low PA doping levels and by $H_4PO_4{}^+$ and H_3PO_4 molecules when the PA doping is higher.

The cause of degradation as function of cell resistivity, PA loss and catalyst agglomeration was investigated by Wannek et al. [6] under different operating conditions. They reported that the loss of acid in PA-doped poly(2,5-benzimidazole) (AB-PBI) membrane was not the main reason for the cell degradation, even when operated at temperatures below 100 °C. The investigation of platinum particle size indicate that the degradation was more dominated by the catalyst. The degradation of start/stop with purging was reported lower compared to cell cycling at 160 over the entire test period [6]. The loss of acid affects the proton conductivity and that leads to cell degradation [11, 7]. Geormezi et al. [12], investigated the effect of PA loading on the anode catalyst when operating with reformed fuel. The study suggests that PA loading needs to be low on the anode catalyst, however the presence of PA assists in faster transfer of protons. Thus, it is seems to be great importance to deduce an optimal doping level for better proton conductivity and longer durability.

The present study aims to map the transient changes in the hydrogen mass transport due to the acid migration towards anode as a function of current density and acid doping. The acid doping effect on acid migration will be important to understand how the performance gets affected and also the optimal acid doping requirement to avoid acid migration and thereby loss of acid and performance.

2. Experimental setup and procedure

The MEAs used in the present study are Dapazol®from Danish Power Systems ApS. The MEA is composed of electrodes on both sides with a thickness of 150 µm and catalyst loading of 1 mg cm^{-2} of platinum. The doping level of the membrane is varied by using three different concentrations of PA and water solution. The concentrations used are (65 %, 75 % and 85 %) for the doping process. The corresponding doping levels were determined as 7, 8.3 and 11 molecules of H_3PO_4 per PBI repeat unit, respectively. The active area of the membrane is 45 cm^2, however, the active area of the electrode was reduced to 2 cm^2, by masking the cathode side membrane using a gasket and having a window of (1.8×1.1) near the cathode outlet open to the gas access. This was done to achieve a uniform flow distribution across the area and to avoid mass transport issues which may arise due to non-uniform flow of gases in the channel. Two channel serpentine and three channel serpentine flow fields were used for the anode and the cathode side, respectively. The gaskets were made of Teflon with a thickness of 150 µm on both sides. The end plates were made of aluminum and the torque applied was 7 N m using 8 tie-rods and spring assembly.

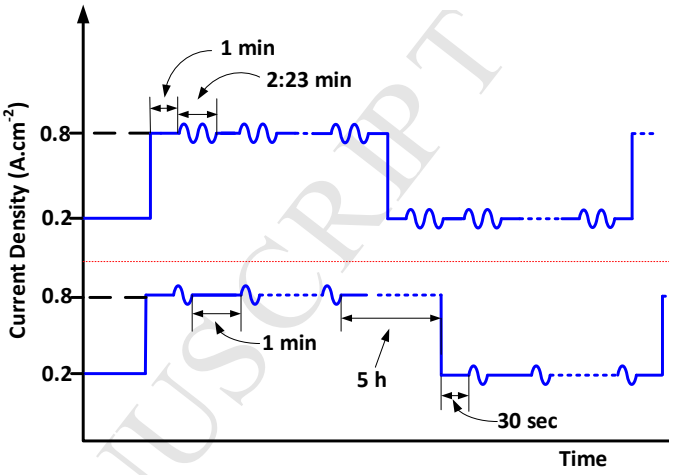

Figure 1: The test sequence of load cycling between 0.2 A cm^{-2} and 0.8 A cm^{-2}, (a) Normal EIS, (b) EIS measurement at one frequency

The tests were carried out with a Greenlight Innovation fuel cell test stand. The electrochemical impedance spectroscopy (EIS) was carried using a Gamry Reference 3000. A break-in process was carried for 100 h at 0.2 A cm^{-2} with hydrogen on the anode and oxygen on the cathode. The flow rates were fixed at 0.2 L min^{-1} and the gases were humidified at room temperature (30 °C) on both sides. The humidification of gases were to avoid the drying of membrane at high flow rate. All experiments were carried out at 160 °C.

The flow rates were fixed at 1 L min^{-1} on both sides for the IV curves as well as the EIS measurements which corresponds to a stoichiometric ratio of above 80 on both sides with pure H_2 and O_2. The test sequence for the experiments are shown in Fig. 1. All the full spectrum EIS measurements were carried out in galvanostatic mode with the amplitude fixed at 5 % of the load and points per decade (ppd) fixed at 5. The points per decade was low in order to reduce the duration of the measurements. The frequency was scanned from 10 kHz to 1 Hz for the complete spectra, while the single frequency measurements were carried out in potenstiostatic mode with a fixed amplitude of 10 mV. The frequency range was restricted to 1 Hz on the lower end to obtain a fast spectra with minimal change in the steady state of the system. Lower frequency was found to take a longer measurement time. The choice of frequency was justified by the fact that mass transport issue was already visible at 1 Hz as seen from Fig. 4. The data validity was ensured using kramer-kronig transformation which showed a error % of less than 1 %. All IV curves were measured by scanning the current at a ramp rate of 0.50 A min^{-1} and the lower voltage limit was set to 0.2 V.

3. Results and discussion

The anode side mass transport is faster due to the lighter H_2 molecules compared to cathode side where the solubility of O_2 in PA is slower [13, 14]. Thus, to determine the mass transport limitations on the anode, the IV curve was recorded under different H_2 concentration on the anode and pure oxygen on the cathode as shown in Fig. 2. To make the gas flow constant for all the IV curves, N_2 was mixed with anode fuel to make it 100 %. The mass transport issues are more dominantly visible for H_2 concentrations below 10 %. A decrease in the limiting current with lower H_2 concentration as seen in Fig. 2 confirms the assumption that mass transport issues are from the anode and not dominated by cathode where oxygen is supplied. The IV curve was used to determine the concentration suitable for cycling the cell between 0.2 and 0.8 A cm^{-2}. Based on the results, to capture the anode mass transport issues on the anode due to acid filling the GDL pores, a concentration of 5 % was chosen. The concentration was chosen such that the voltage was above 0.4 V for both 0.2 and 0.8 A cm^{-2}. A lower concentration of anode fuel was used to make the mass transport issue on the anode more dominant. The low concentration also simulates the scenario, where some areas on the catalyst have a very low H_2 concentration when operating with reformed fuel.

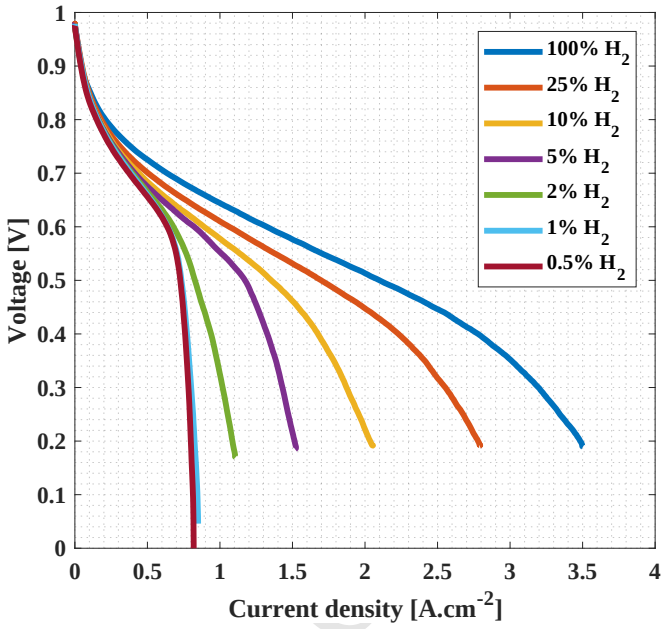

Figure 2: IV curve at different H_2 concentrations.

The first experiment was carried out with MEAs doped with 85 % concentrated PA and a doping level of 11 molecules of H_3PO_4 per PBI repeat unit. The EIS recorded with an interval of 1 min is shown in Fig. 3. The EIS was recorded after changing the current to 0.8 A cm^{-2} and 1 min rest time after an operation of ≈5 h at 0.2 A cm^{-2}. The anode fuel concentration was fixed at 5 % H_2 and 95 % N_2 during the tests. The measurement time for each EIS spectrum was 2 min and 23 s. The results indicate no significant difference in the EIS spectra when changing from high to low current density.

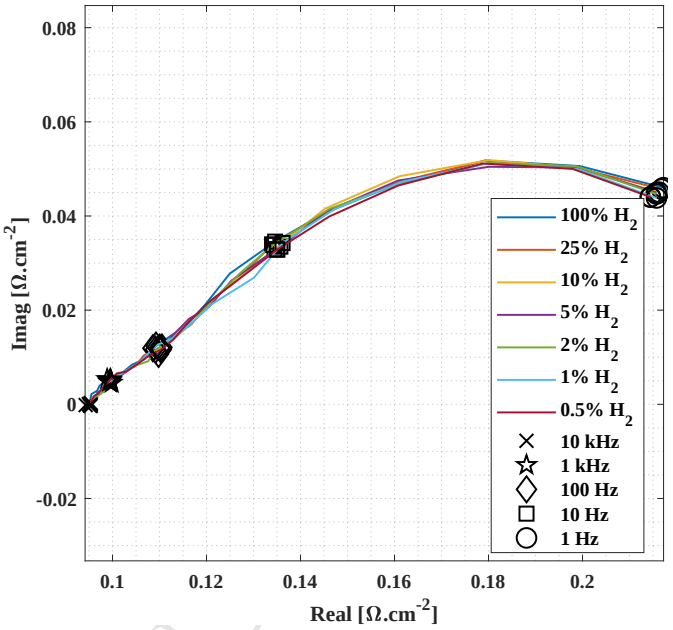

Figure 3: EIS over time at 0.2 A cm^{-2} with 5 points per decade

The analysis of EIS data shows no or minimal differences in the spectra over time. This suggests that acid migration from the membrane to the anode GDL (if any), which is assumed to affect the mass transport issue is not captured by the full spectra EIS measurement. However, based on previous experience and results from [15], it is known that acid migration and redistribution is a fast process and the time taken to record the EIS could be too long for detecting the acid kinetics related phenomena.

The EIS interpretations in the literature [16, 17] suggests that the mass transport issues are dominant in the low frequency region <10 Hz of the EIS spectra. Thus, to reduce the measurement time and be able to detect the fast acid kinetics related mass transport issues on the anode, the range of frequency scan was reduced. A frequency range from 10 Hz to 0.5 Hz with 5 points per decade was selected. The EIS recorded is shown in Fig. 4. The impedance at frequencies below 1.6 Hz shows an increase over time at 0.2 A cm^{-2}. While at high current density (0.8 A cm^{-2}), the points overlap. This suggests that change of current density has an effect on the low frequency resistance which is mainly contributed by the mass transport issues [17, 16]. However, when a similar measurement is carried out at high current density, the mass transport issues are not visible or not captured by the fast frequency scan. This could be either due to fast acid kinetics at high current density or the noise in the measurement at high current density (low voltage) is shadowing the small resistance change at low frequency.

Thus, the next step was to carry out impedance measurement at a single frequency. The cell was operated at one current density for 5 h before changing the current density and starting the measurements. This was to make sure that the acid-water balance within the system has reached a uniform distribution within the cell. The measurements were repeated for three cycles and the mean value was plotted. This was to eliminate

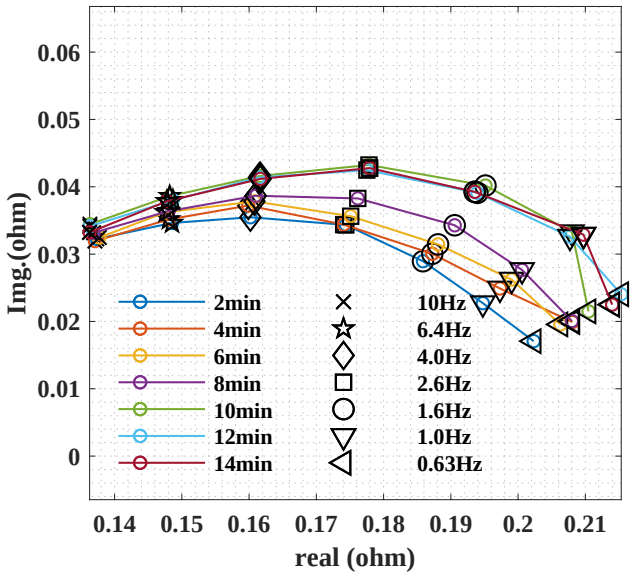

(a) Low frequency (10 to 0.5 Hz) EIS recorded over time at 0.2 A cm^{-2}

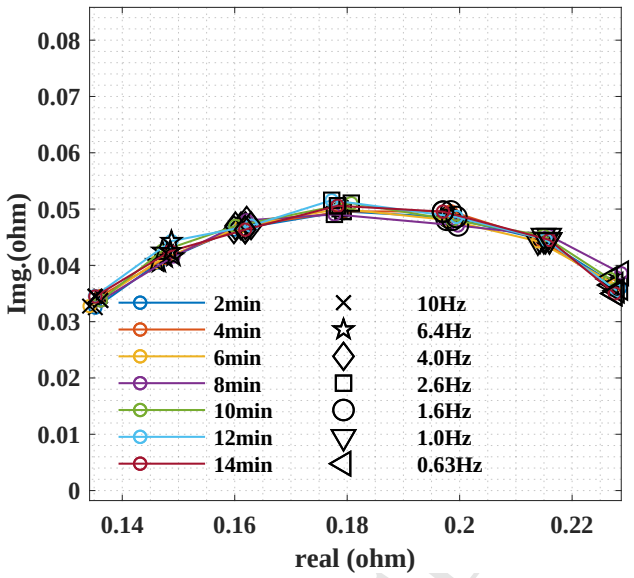

(b) Low frequency (10 to 0.5 Hz) EIS recorded over time at 0.8 A cm^{-2}

Figure 4: Low frequency (10 to 0.5 Hz) EIS recorded over time at 0.2 A cm^{-2} and 0.8 A cm^{-2}

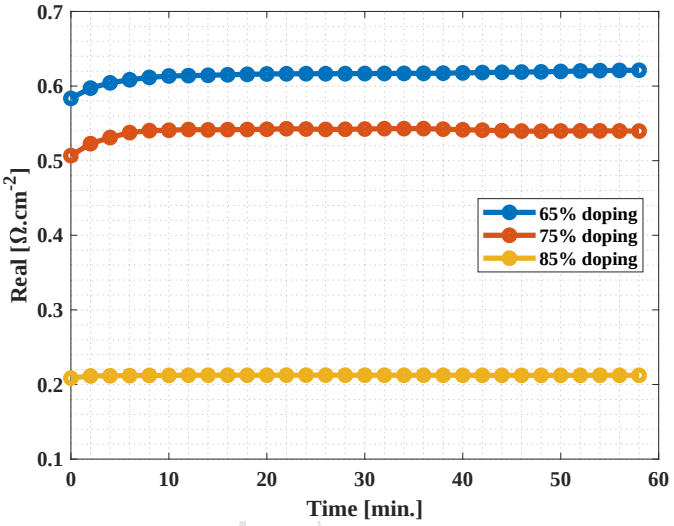

(a) Resistance change over time at 0.2 A cm^{-2}

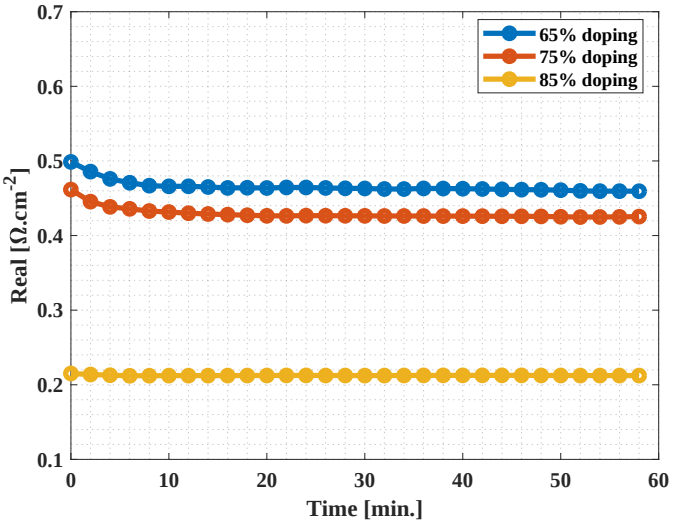

(b) Resistance change over time at 0.8 A cm^{-2}

Figure 5: Low frequency resistance change over time at @ 0.2 A cm^{-2} and 0.8 A cm^{-2}

the experimental error and to have a statistical validation of the data.

In Fig. 5 (a), the resistance at 1 Hz measured for 1 h at 0.2 A cm^{-2} is shown. An increase in resistance at the beginning is measured and then it stabilizes. The resistance for three different doping levels also show a difference in the low frequency resistance. A lower doping level has a higher resistance and the difference is quite significant. These differences are attributed to the acid doping which probably results in a variation in the absolute value of the resistance for the differently doped MEAs.The MEA with a doping of 7 molecules of H_3PO_4 per PBI repeat unit has the highest resistance. An increase in the doping to 8.3 and 11 molecules of H_3PO_4 per PBI repeat unit resulted in a decrease in the resistance. This indicates that the performance also has a direct correlation to the doping of the MEA.

Similarly, the resistance over time measured at 0.8 A cm^{-2} is shown in Fig. 5 (b). The resistance decreases over time for high current density operation at the beginning and then the resistance stabilizes. The 1 Hz frequency resistance over time shows an increase at low current density (0.2 A cm^{-2}) and decrease at high current density (0.8 A cm^{-2}). The resistance changes are seen to be minimal for a doping level of 11 molecules of H_3PO_4 per PBI repeat unit. This suggests that the optimal doping level for minimal acid redistribution is around 11 molecules of H_3PO_4 per PBI repeat unit.

The comparison of plots in Fig. 5 (a) and (b) for each dop-

ing level show a variation in the difference between the two current densities. The shrinking of impedance as the current increase is because of the change of slope on the IV curve, which is equivalent to the low frequency intercept of the impedance spectra with the real axis [18]. Thus, at higher current the low frequency resistance should be lower compared to at lower current density. However, in this case the doping level-based slope change could be seen. The lowest doping level show maximum difference between the two current densities low frequency resistance which corresponds to the IV curve slope. This difference could be attributed to low PA doping level results in a scarcity of proton conductors which becomes dominant at high current density compared to low current density.

The difference between the initial resistance at 0.2 A cm^{-2} and the initial resistance at 0.8 A cm^{-2} for each doping level was calculated to deduce the difference in the resistance. The percentage change in resistance with current density was calculated as 3.5 %, 9.8 % and 17 % for doping levels of 11, 8.3 and 7 molecules of H_3PO_4 per PBI repeat unit, respectively. This difference suggest that the change of resistance over time is slower for a doping level of 11 molecules of H_3PO_4 per PBI repeat unit compared to other lower doping levels of 8.3 and 7 molecules of H_3PO_4 per PBI repeat unit.

The above two arguments suggest that the voltage change with current density is different for the differently doped MEAs. This is of interest to predict the performance of HT-PEMFCs with differently doped PBI membranes.

4. Discussion

To map the doping level, transient hydrogen mass transport resistance and current density, the resistance was fitted with a function as defined by Eqn. 1. The variable 'b' in the equation represent the time constant for the linear time varying system to reach steady state when a change in the input was initiated. The change in the present case was current density while all the other parameters were kept constant.

$$f(x) = a \times e^{(\frac{-x}{b})} + c \tag{1}$$

where a and c are constants and b is the time constant of function 'f'.

The current density change induces a variation in the PA distribution which in turn changes the output resistance of the system. A current density induced changes in PA distribution in an HT-PEMFC was also reported in [19, 20, 21].

The fitted resistance for different PA loading and two current densities, 0.2 and 0.8 A cm^{-2} are shown in Fig. 6 (a), (b) and (c). The trend shows increase in resistance at 0.2 A cm^{-2} and a decrease in resistance at 0.8 A cm^{-2} for all the three differently doped MEAs.

In Fig.6 (a) shows the resistance change over time for an MEA with a doping level of 11 molecules of H_3PO_4 per PBI repeat unit. The time constants for low and high current densities are 2 and 2.5 minutes, respectively. The resistance becomes stable very fast indicating that the acid redistribution is a fast process. However, from the resistance changes shown in

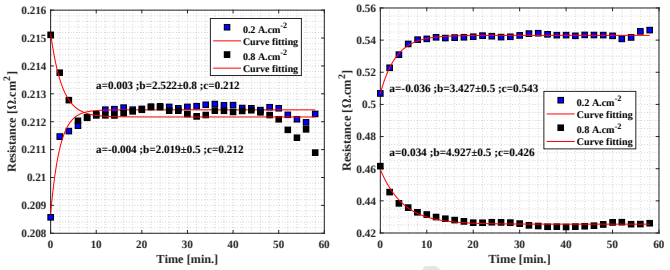

(a) 11 molecules of H_3PO_4 per PBI repeat unit

(b) 8.3 molecules of H_3PO_4 per PBI repeat unit

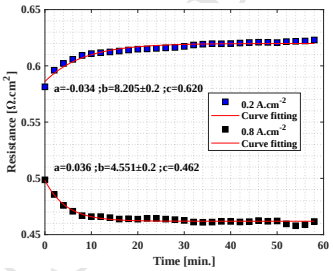

(c) 7 molecules of H_3PO_4 per PBI repeat unit

Figure 6: Fitted resistances showing the time constants at 0.2 A cm^{-2} and at 0.8 A cm^{-2} for differently doped MEAs

Fig.6 (b) and (c) for doping levels of 8.3 and 7 molecules of H_3PO_4 per PBI repeat unit, respectively, the time constants are longer.

The time constants for MEAs with different loading show an increasing trend with a decrease in the acid loading. In the case of high current density operation, the time constants are similar for a loading of 8.3 and 7 molecules of H_3PO_4 per PBI repeat unit and was calculated to be around 4.5 minutes. While in the case of low current density operation a clear variation in the time constant was calculated. The time constant for lowest loading of 7 molecules of H_3PO_4 per PBI repeat unit was highest and vice verse for higher loadings of 8.3 and 11 molecules of H_3PO_4 per PBI repeat unit.

In literature [19, 22] it was reported that at high current densities the acid/water migrates from the cathode to the anode and back-diffuses at low current densities. The acid/water migrating to the anode builds up a capillary force due to change in the concentration of PA, which pushes the acid into the GDL and thereby hinders the pathway for the H_2. The opposite happens at lower current densities.

However, in the present case the acid doping level is 3 times lower compared to the one reported in [19], and hence, seems to behave in a different way. At low current density the low frequency resistance increases and at high current density the low frequency resistance decreases. This could be seen from Fig.6 (a), (b) and (c).

Becker et al. [21] used MEAs with doping level similar to the present study. They reported the acid is migrating from the cathode to the anode at high current density and back-diffusion happens at low current density using ohmic resistance measure-

ment of the membrane. They reported a balancing of back diffusion and migration could be achieved with proper doping levels and width of the membrane. The relationship of back diffusion at steady-state is calculated using Fick's law of diffusion as shown in Eqn. 2. A higher doping level increases back-diffusion and thinner membrane facilitates faster back-diffusion.

$$J_m = D \times \Delta[H_3PO_4]/w \quad (2)$$

where J_m is the diffusion flux, D is the diffusion coefficient, $\Delta[H_3PO_4]$ is the change in concentration and w is the thickness of the membrane.

A lower acid concentration also results in a thinner membrane, i.e., lower 'w' in Eqn.2 compared to higher doped MEAs, which swells with the acid uptake. Thus, the back-diffusion could be faster depending on which parameter of the two mentioned above is more dominant.

The migration of acid from the membrane to the anode catalyst may take place under high current density operation and the generated capillary force, which facilitates the drag of acid to the GDL, is lower when the doping level is lower. Due to the low acid doping, the concentration distribution of acid in the catalyst layer is possibly lower. Therefore, the migration of acid/water towards the anode facilitates the formation of more active three phase boundary closer to the catalyst active sites. Hence H_2 access to the three phase boundary becomes easier and the transport of generated proton also becomes easier provided the acid has a connectivity to the membrane. This assumption is valid as many have reported the strong interaction of acid and PBI [23]. Another possibility is the influence of higher water generation leads to better proton conductivity through the membrane. The paper focuses on determining an optimal acid doping level for HT-PEMFCs for longer durability under varying load operations. The manuscript suggests that acid loss which is a major issue in HT-PEMFC could be solved using an optimal doping level. The manuscript focusses on load cycling profile which fits well with automotive as well as stationary power systems drives. As such, this paper should be of interest to a broad readership including those interested in system design: High temperature Polymer Electrolyte Membrane Fuel Cells: EIS modelling, testing, and performance characterization. Thank you for your consideration of our work. Please address all correspondence concerning this manuscript to me at the Aalborg University and feel free to correspond with me by e-mail (sot@et.aau.dk). Some of the potential reviewers who work on similar topics are mentioned below.

The calculated time constants for the resistances to become stable are shown in Table 1.

In the present case, the flow rates are 1 L min^{-1} on both sides, which corresponds to a stoichiometric ratio of above 80 on both sides with pure H_2 and O_2. Thus, the change in resistance arising due to cathode flow variation seems unlikely.

The three doping levels have different time constant of rising and falling resistance at low and high current densities. The highest time constants are for the MEAs with the least doping level. These time constants are calculated by fitting the mean of three measurements of each current density. This is a clear

Table 1: Time constants taken for the resistance to become stable at 0.2 A cm^{-2} and 0.8 A cm^{-2}

Acid doping molecules of PA per PBI repeat unit	Time constant (at 0.2 A cm^{-2}) [min]	Time constant (at 0.8 A cm^{-2}) [min]
11	2.0±0.5	2.5±0.8
8.3	3.4±0.3	4.9±0.3
7	8.2±0.2	4.5±0.2

indication that the acid movement dynamics are influenced by the doping level.

To understand the phenomena better, the resistance at 1 kHz was recorded over time. The ohmic resistance also follows the same trend as the low frequency resistance as shown in Fig. 7. A similar result was reported in [22]. They saw an increase in high frequency intercept when the current was switched off and then an decrease in HFR when current was applied. They explained the phenomena based on hydration/dehydration of PA in the membrane. The resistance change at high frequency was determined for the MEA with 8.3 molecules of H_3PO_4 per PBI repeat unit. The time constants were calculated as 5.4 and 1.1 minute for high and low current density operation.

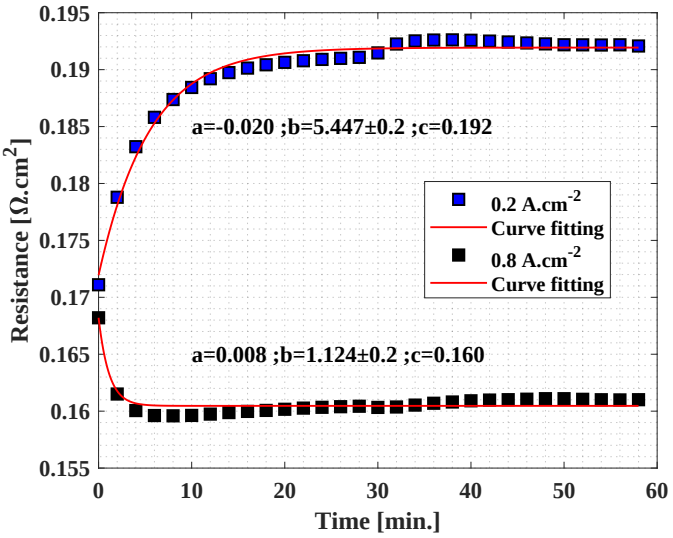

Figure 7: Ohmic resistance at 1 kHz over time at 0.2 A cm^{-2} and 0.8 A cm^{-2}

Thus, the increases and decreases of high frequency intercept suggests that the low frequency resistance trends with current density and doping level could be an influence of the HFR intercept being transmitted in the impedance spectrum.

A lower doping level is seen to have a higher absolute resistance values and thus, the performance will be lower. On the other hand, a lower doping level is seen to reduce the loss of acid higher as the resistance is seen to be continuously decreasing with time at 0.8 A cm^{-2}. Thus, a comparison of different resistances at low and high frequency and also at different doping levels and current density suggest that doping level of 11

molecules of H_3PO_4 per PBI repeat unit is optimal for better performance and longer durability.

5. Conclusion

Three MEAs with doping levels of 11, 8.3 and 7 molecules of H_3PO_4 per PBI repeat unit were investigated with EIS and modified EIS methods. The objective was to map the doping level, current density and transient H_2 mass transport resistance. A low current density of 0.2 A cm^{-2} and a high current density of 0.8 A cm^{-2} was selected for inducing a change in the acid dynamics. The tests were carried out to quantify issues related to acid/water migrating towards the anode at high current density and back-diffusion when operating at low current density. The impedance at two different frequencies, high and low was used to quantify the process occurring at the anode. To ensure that the anode limitations are recorded at low frequency, the cathode was supplied with pure oxygen at a high stoichiometry and the anode supply was 5 % H_2 and 95 % N_2 mixture. The assumption here was the low H_2 concentration would enhance the anode effect and at the same time simulate the concentration at some portions of a fuel cell operating with reformed fuel.

At low current density the resistance at 1 Hz frequency and at 10 kHz increased immediately for a short time before getting stabilised. While on the other hand at high current density the resistance at both high and low frequency decreased before stabilizing. The low frequency region which is associated with mass transport (in this case H_2 mass transport) improved when the current was high for a short time before stabilizing and it degraded when the current was low.

The time constants for these changes in resistance were calculated as 2.0±0.5, 3.4±0.3 and 8.2±0.2 min at 0.2 A cm^{-2}, and 2.5±0.8, 4.9±0.3 and 4.5±0.2 min at and 0.8 A cm^{-2} for 11, 8.3 and 7 molecules of H_3PO_4 per PBI repeat unit, respectively.

The high frequency resistance measurement suggest that the changes seen in the low frequency are dominantly influenced by the changes in the proton conductivity of the membrane and the mass transport is not influenced by the current density when the doping levels are around ≈11 molecules of H_3PO_4 per PBI repeat unit. This is an interesting finding as it suggest that when the doping level is low, the GDL flooding and thereby loss of acid by evaporation is not a major issue in the durability of HT-PEMFC operating under load cycles. Another interesting aspect which was deduced based on the current experimental results is the optimal acid doping level for HT-PEMFC to operate with minimal acid loss is somewhere around 11 molecules of H_3PO_4 per PBI repeat unit as higher doping level of around 33 molecules of H_3PO_4 per PBI repeat unit has been investigated by others [5], and have suggest flooding of GDL and thereby induced acid losses. This is important in cases of automotive applications were the drive cycle involves cycling of load. Thus, a doping level of around 11 molecules of H_3PO_4 per PBI repeat unit could provide with a longer durability when cycling of load is involved.

Acknowledgement

The authors would like to thank the Innovation Fund Denmark for funding the work through the 4M project. The authors are also thankful to Danish Power Systems for providing the MEA used in the experiment.

References

References

[1] Thomas J Schmidt. Durability and Degradation in High-Temperature Polymer Electrolyte Fuel Cells. *ECS Transactions*, 1(8):19–31, jun 2006. doi: 10.1149/1.2214541. URL http://ecst.ecsdl.org/content/1/8/19.abstract.

[2] Samuel Simon Araya, Fan Zhou, Vincenzo Liso, Simon Lennart Sahlin, Jakob Rabjerg Vang, Sobi Thomas, Xin Gao, Christian Jeppesen, and Søren Knudsen Kær. A comprehensive review of PBI-based high temperature PEM fuel cells. *International Journal of Hydrogen Energy*, 41(46): 21310–21344, 2016. ISSN 03603199. doi: 10.1016/j.ijhydene.2016.09.024.

[3] Jakob Rabjerg Vang, Søren Juhl Andreasen, Samuel Simon Araya, Søren Knudsen Kær, Samuel Simon Araya, and Søren Knudsen Kær. Comparative study of the break in process of post doped and sol–gel high temperature proton exchange membrane fuel cells. *International Journal of Hydrogen Energy*, 39(27):14959–14968, sep 2014. ISSN 03603199. doi: 10.1016/j.ijhydene.2014.07.017. URL http://www.sciencedirect.com/science/article/pii/S0360319914019727.

[4] Yuka Oono, Atsuo Sounai, and Michio Hori. Long-term cell degradation mechanism in high-temperature proton exchange membrane fuel cells. *Journal of Power Sources*, 210:366–373, jul 2012. ISSN 03787753. doi: 10.1016/j.jpowsour.2012.02.098. URL http://www.sciencedirect.com/science/article/pii/S0378775312005204.

[5] S. H. Eberhardt, T. Lochner, F. N. Büchi, and T. J. Schmidt. Correlating Electrolyte Inventory and Lifetime of HT-PEFC by Accelerated Stress Testing. *Journal of The Electrochemical Society*, 162(12):F1367–F1372, sep 2015. ISSN 0013-4651. doi: 10.1149/2.0591512jes. URL http://jes.ecsdl.org/lookup/doi/10.1149/2.0591512jes.

[6] C. Wannek, B. Kohnen, H. F. Oetjen, H. Lippert, and J. Mergel. Durability of ABPBI-based MEAs for high temperature PEMFCs at different operating conditions. *Fuel Cells*, 8(2):87–95, 2008. ISSN 16156846. doi: 10.1002/fuce.200700059.

[7] S Yu, L. Xiao, and B. C. Benicewicz. Durability Studies of PBI-based High Temperature PEMFCs. *Fuel Cells*, 8(3–4):165–174, jul 2008. ISSN 16156846. doi: 10.1002/fuce.200800024. URL http://doi.wiley.com/10.1002/fuce.200800024.

[8] Wiebke Maier, Tobias Arlt, Christoph Wannek, Ingo Manke, Heinrich Riesemeier, Philipp Krüger, Joachim Scholta, Werner Lehnert, John Banhart, and Detlef Stolten. In-situ synchrotron X-ray radiography on high temperature polymer electrolyte fuel cells. *Electrochemistry Communications*, 12(10):1436–1438, oct 2010. ISSN 13882481. doi: 10.1016/j.elecom.2010.08.002. URL http://www.sciencedirect.com/science/article/pii/S1388248110003474.

[9] Yuichi Aihara, Atsuo Sonai, Mineyuki Hattori, and Kikuko Hayamizu. Ion conduction mechanisms and thermal properties of hydrated and anhydrous phosphoric acids studied with1H, 2H, and31P NMR. *Journal of Physical Chemistry B*, 110(49):24999–25006, dec 2006. ISSN 15206106. doi: 10.1021/jp064452v. URL http://www.ncbi.nlm.nih.gov/pubmed/17149922.

[10] Th Dippel, K. D. Kreuer, J. C. Lassègues, and D. Rodriguez. Proton conductivity in fused phosphoric acid; A 1H/31P PFG-NMR and QNS study. *Solid State Ionics*, 61(1-3):41–46, 1993. ISSN 01672738. doi: 10.1016/0167-2738(93)90332-W.

[11] Yunfeng Zhai, Huamin Zhang, Gang Liu, Jingwei Hu, and Baolian Yi. Degradation Study on MEA in H[sub 3]PO[sub 4]PBI High-Temperature PEMFC Life Test. *Journal of The Electrochemical Society*, 154(1):B72, jan 2007. ISSN 00134651. doi: 10.1149/1.2372687. URL http://jes.ecsdl.org/cgi/doi/10.1149/1.2372687.

[12] Maria Geormezi, Fotis Paloukis, Alin Orfanidi, Nivedita Shroti, Maria K. Daletou, and Stylianos G. Neophytides. The structure and stability of the anodic electrochemical interface in a high temperature polymer electrolyte membrane fuel cell under reformate feed. *Journal of Power Sources*, 285:499–509, 2015. ISSN 03787753. doi: 10.1016/j.jpowsour.2015.03.109. URL http://dx.doi.org/10.1016/j.jpowsour.2015.03.109.

[13] Maria Geormezi, Fotis Paloukis, Alin Orfanidi, Nivedita Shroti, Maria K. Daletou, and Stylianos G. Neophytides. The structure and stability of the anodic electrochemical interface in a high temperature polymer electrolyte membrane fuel cell under reformate feed. *Journal of Power Sources*, 285:499–509, 2015. ISSN 03787753. doi: 10.1016/j.jpowsour.2015.03.109. URL http://dx.doi.org/10.1016/j.jpowsour.2015.03.109.

[14] Zhenyu Liu, Jesse S. Wainright, Morton H. Litt, and Robert F. Savinell. Study of the oxygen reduction reaction (ORR) at Pt interfaced with phosphoric acid doped polybenzimidazole at elevated temperature and low relative humidity. *Electrochimica Acta*, 51(19):3914–3923, may 2006. ISSN 00134686. doi: 10.1016/j.electacta.2005.11.019. URL http://www.sciencedirect.com/science/article/pii/S0013468605012922.

[15] S. H. Eberhardt, F. Marone, M. Stampanoni, F. N. Büchi, and T. J. Schmidt. Quantifying phosphoric acid in high-temperature polymer electrolyte fuel cell components by X-ray tomographic microscopy. *Journal of Synchrotron Radiation*, 21(6):1319–1326, nov 2014. ISSN 1600-5775. doi: 10.1107/S1600577514016348. URL http://www.ncbi.nlm.nih.gov/pubmed/25343801http://scripts.iucr.org/cgi-bin/paper?S1600577514016348.

[16] Sobi Thomas, Jakob Rabjerg Vang, Samuel Simon Araya, and Søren Knudsen Kær. Experimental study to distinguish the effects of methanol slip and water vapour on a high temperature PEM fuel cell at different operating conditions. *Applied Energy*, 192:422–436, apr 2016. ISSN 0306-2619. doi: http://dx.doi.org/10.1016/j.apenergy.2016.11.063. URL http://linkinghub.elsevier.com/retrieve/pii/S0306261916316488http://www.sciencedirect.com/science/article/pii/S0306261916316488.

[17] S. M. Rezaei Niya, R. K. Phillips, and M. Hoorfar. Sensitivity Analysis of the Impedance Characteristics of Proton Exchange Membrane Fuel Cells. *Fuel Cells*, 16(5):547–556, jul 2016. ISSN 16156854. doi: 10.1002/fuce.201600060. URL http://doi.wiley.com/10.1002/fuce.201600060.

[18] M. Chandesris, C. Robin, M. Gerard, and Y. Bultel. Investigation of the difference between the low frequency limit of the impedance spectrum and the slope of the polarization curve. *Electrochimica Acta*, 180:581–590, oct 2015. ISSN 00134686. doi: 10.1016/j.electacta.2015.08.089. URL http://linkinghub.elsevier.com/retrieve/pii/S001346861530339X.

[19] S. H. Eberhardt, M. Toulec, F. Marone, M. Stampanoni, F N Büchi, T. J. Schmidt, F. N. Buchi, and T. J. Schmidt. Dynamic Operation of HT-PEFC: In-Operando Imaging of Phosphoric Acid Profiles and (Re)distribution. *Journal of The Electrochemical Society*, 162(3):F310–F316, jan 2015. ISSN 0013-4651. doi: 10.1149/2.0751503jes. URL http://jes.ecsdl.org/content/162/3/F310.abstracthttp://jes.ecsdl.org/cgi/doi/10.1149/2.0751503jes.

[20] S. H. Eberhardt, F. Marone, M. Stampanoni, F. N. Büchi, and T. J. Schmidt. Operando X-ray Tomographic Microscopy Imaging of HT-PEFC: A Comparative Study of Phosphoric Acid Electrolyte Migration. *Journal of The Electrochemical Society*, 163(8):F842–F847, jun 2016. ISSN 0013-4651. doi: 10.1149/2.0801608jes. URL http://jes.ecsdl.org/lookup/doi/10.1149/2.0801608jes.

[21] Hans Becker, Lars Nilausen Cleemann, David Aili, Jens Oluf Jensen, and Qingfeng Li. Probing phosphoric acid redistribution and anion migration in polybenzimidazole membranes. *Electrochemistry Communications*, 82 (July):21–24, 2017. ISSN 13882481. doi: 10.1016/j.elecom.2017.07.005. URL http://dx.doi.org/10.1016/j.elecom.2017.07.005.

[22] K. Wippermann, C. Wannek, H.-F. Oetjen, J. Mergel, and W. Lehnert. Cell resistances of poly(2,5-benzimidazole)-based high temperature polymer membrane fuel cell membrane electrode assemblies: Time dependence and influence of operating parameters. *Journal of Power Sources*, 195(9):2806–2809, may 2010. ISSN 03787753. doi: 10.1016/j.jpowsour.2009.10.100. URL http://www.sciencedirect.com/science/article/pii/S0378775309019776.

[23] R Zeis. Materials and characterization techniques for high-temperature polymer electrolyte membrane fuel cells. *Beilstein Journal of Nanotechnology*, 2015. URL http://www.beilstein-journals.org/bjnano/content/html/2190-4286-6-8.html.

Highlights

- Enhanced durability of HT-PEMFC under load cycling drive cycle.
- Mitigation of Phosphoric acid migration towards anode with optimal acid doping.
- Modified impedance to distinguish different loss in HT-PEMFC.
- Phosphoric acid dynamics calculated under load cycling.